

Chorion formation in panoistic ovaries requires windei and trimethylation of histone 3 lysine 9

Herraiz, A., Belles X., Piulachs MD*.

Institute of Evolutionary Biology (CSIC-Universitat Pompeu Fabra), Passeig Maritim de la Barceloneta 37-49, 08003 Barcelona, Spain.

A.H.: alba.herraiz@ibe.upf-csic.es ; X.B.: xavier.belles@ibe.upf-csic.es ; M.D.P.: mdolors.piulachs@ibe.upf-csic.es

*Corresponding:

Maria-Dolors Piulachs

Institute of Evolutionary Biology (CSIC-Universitat Pompeu Fabra), Passeig Maritim de la Barceloneta 37-49, 08003 Barcelona, Spain.

E-mail: mdolors.piulachs@ibe.upf-csic.es

Phone: + 34 93 230 96 48

Fax: + 34 93 221 10 11

Abstract

Epigenetic modifications play key roles in transcriptional regulation. Trimethylation of histone 3 lysine 9 (H3K9me3) is one of the most widely studied histone post-translational modifications, and has been linked to transcriptional repression. In *Drosophila melanogaster*, Windei is needed for H3K9me3 in female germ line cells. Here we report the occurrence of a *D. melanogaster* Windei (Wde) ortholog in the ovary of the hemimetabolous insect *Blattella germanica*, which we named BgWde. Depletion of BgWde by RNAi reduced H3K9me3 in follicular cells, which triggered changes in transcriptional regulation that led to the prevention of chorion genes expression. In turn, this impaired oviposition (and the formation of the ootheca) and, therefore, prevented reproduction. Windei and H3K9me3 have already been reported in follicular cells of *D. melanogaster*, but this is the first time that the function of these modifications has been demonstrated in the said cells. This is also the first time that an epigenetic mark is reported as having a key role in choriogenesis.

Keywords: *Blattella germanica*, H3K9me3, follicular epithelia, *Drosophila*, oogenesis

1. Introduction

Although every somatic cell of a given eukaryote has the same DNA sequence, gene expression can vary a lot between different cell types and under different conditions in a given cell type. Precisely regulated gene expression is needed to maintain cell identity and to respond to developmental and environmental signals. Chromatin modifications, such as DNA methylation and histone post-translational modifications (PTMs), play a key role in this precise regulation of gene expression. DNA methylation occurs in cytosine residues and generally impairs transcription, whereas histone PTMs have been related with both transcriptional repression and activation [1, 2]. Histones are subjected to several PTMs, like acetylation, phosphorylation, methylation, ubiquitination and ADP-ribosylation [3]. The functional consequences of these modifications can be direct, causing structural changes to chromatin, or indirect, acting through the recruitment of effector proteins [2]. The occurrence of lysine methylation in histone 3 (H3) and histone 4 (H4) tails has important consequences in many biological processes, including heterochromatin formation, X-chromosome inactivation and transcriptional regulation [4]. Six lysine-methylation sites have been identified to date: K4, K9, K27, K36 and K79 in H3 and K20 in H4. In addition, the lysine residue can be mono-, di-, or trimethylated, and this differential methylation provides further functional diversity to the site [5]. Methylation of lysine 9 in H3 (H3K9) has been thoroughly studied, as it plays a crucial role in heterochromatin formation and maintenance, as well as in gene silencing [6]. In 2003, Wang and coworkers demonstrated that the protein mAM/MCAF1 facilitates the conversion of dimethyl-H3K9 to trimethyl- H3K9 by the histone methyl transferase ESET/SETDB1 in human HeLa cells [7]. Six years later, Koch and colleagues showed that an ortholog of mAM/MCAF1 in *Drosophila melanogaster*, which they named Windei, is essential for trimethylation of H3K9 (H3K9me3) by dSETDB1/Eggless, the only histone methyl transferase that is essential for egg viability and fertility [8].

In *D. melanogaster*, H3K9me3 is present in the ovary in both germ and somatic cells, and is required for oogenesis [9]. Several authors have highlighted the key role of H3K9me3 in germ line cells in *D. melanogaster* [8, 10, 11], but practically nothing is known about its function in follicular cells.

The present study reports the occurrence of an ortholog of the mammalian mAM/MCAF and the *D. melanogaster* Windei in the ovary of the hemimetabolous insect *Blattella germanica*. This cockroach has panoistic ovaries, which is the least modified insect ovarian type. In each gonadotrophic cycle only the basal follicles mature, at the end of maturation the follicular cells secrete the chorion and the eggs are oviposited in an egg-case or ootheca. The process of choriogenesis occurs at day 7 of the adult life and lasts around 15 h. It can be divided into three different stages, early choriogenesis (EC), mid choriogenesis (MC), and late choriogenesis (LC). At the end of the process, the complete chorion structure has a complex basal endochorion (composed of a thin inner endochorion, which stands on the vitelline membrane, a thick columnar layer and an outer endochorion) and an apical layer called the exochorion [12, 13]. Here we show that Windei is required for H3K9me3 in the follicular cells of *B. germanica* and that in the absence of Windei, chorion layers do not develop and eggs are not oviposited.

2. Material and Methods

2.1. Insect colony and tissue sampling

Sixth instar nymphs or adult females of *B. germanica* were obtained from a colony fed on Panlab dog chow and water *ad libitum*, and reared in the dark at $29\pm 1^\circ\text{C}$ and 60–70% relative humidity. In adult females the length of the basal oocyte was used to stage the ovaries from 0- to 7-day-old, according to [12]. Three-day-old adult females were maintained with males during all the first gonadotrophic cycle, and mating was confirmed at the end of the experiments by assessing the presence of spermatozoa in the spermatheca. All dissections and tissue sampling were carried out on carbon dioxide-anaesthetized specimens. Tissues used in the experiments were the following: ovaries, brain, fat body abdominal lobes, levator and depressor muscles of tibia, digestive tract from the pharynx to the rectum (Malpighian tubules excluded), isolated Malpighian tubules and colleterial glands. After the dissection, the tissues were frozen in liquid nitrogen and stored at -80°C until use.

2.2. Cloning and sequencing

Two non-overlapping fragments of 473 and 540 bp corresponding to the *Windei* ortholog of *B. germanica* (BgWde) were obtained from an ovarian cDNA subtractive library previously carried out in our laboratory [14]. To complete the sequence, conventional RT-PCRs, as well as 3'- and 5'-rapid amplifications of cDNA ends (RACE) were applied to ovarian cDNA using FirstChoice® RLM-RACE (Ambion, Huntingdon, Cambridgeshire, UK), according to the manufacturer's instructions. The amplified fragments were analyzed by agarose gel electrophoresis, cloned into the pSTBlue-1 vector (Novagen, Madison, WI, USA) and sequenced. Primers used are detailed in Supplementary Table 1.

2.3. RNA extraction and retrotranscription to cDNA

All RNA extractions were performed using the Gen Elute Mammalian Total RNA kit (Sigma, Madrid, Spain). RNA quantity and quality were estimated by spectrophotometric absorption at 260 nm/280nm in a Nanodrop Spectrophotometer ND-1000® (NanoDrop Technologies, Wilmington, DE, USA). A sample of 400 ng of total RNA from each extraction was DNase treated (Promega, Madison, WI, USA) and reverse transcribed with Transcriptor First Strand cDNA Synthesis Kit (Roche, Sant Cugat del Valles, Barcelona, Spain). In all cases we followed the manufacturer's protocols.

2.4. Expression studies

Expression of BgWde in different tissues was studied by semiquantitative PCR using the following conditions: 94°C for 2 min, then 35 cycles at 94°C for 30 sec, 58°C for 30 sec, and 72°C for 30 sec and a final extension of 7 min. The actin-5c gene of *B. germanica* was used as a reference.

Quantitative real-time PCR (qRT-PCR) was used to study BgWde expression in ovary during the last nymphal instar and the first gonadotrophic cycle and to assess the effect of BgWde depletion. qRT-PCR reactions were carried in an iQ5 Real-Time PCR Detection System (Bio-Rad Laboratories, Madrid, Spain), using IQ™ SYBR Green

Supermix (BioRad). The actin-5c gene of *B. germanica* was used as a reference. The efficiency of primers was first validated by constructing a standard curve through four serial dilutions of cDNA from ovaries. At least three independent qRT-PCR experiments (biological replicates) were performed, and each measurement was done in triplicate (technical replicates). qRT-PCR reactions were performed and analyzed as previously described [15]. Fold change expression was calculated using the REST-2008 program [Relative Expression Software Tool V 2.0.7; Corbett Research [16]]. PCR primers used in qRT-PCR expression studies were designed using the Primer Express 2.0 software (Applied Biosystems, Foster City, CA, USA), and are indicated in Supplementary Table 1.

Together with actin-5c (GenBank: *AJ862721*) and windei (GenBank: *HF969270*), we studied the expression of follicle cell protein 3C (Fcp3C; GenBank: *FM253348.1*), yellow-g (GenBank: *FM210754.1*), citrus (GenBank: *FN823078.1*), brownie (GenBank: *FN429652.1*) [13, 14, 17], lipid storage droplet-2 (Lsd-2; GenBank: *HF969269*), origin recognition complex subunit 1 (orc1; GenBank: *HF969268*) and cyclin E (GenBank: *HF969267*). We also analyzed the expression of hippo (GenBank: *HF969251*), yorkie (GenBank: *HF969252*), notch (GenBank: *HF969255*), hindsight (GenBank: *HF969258*), and cut (GenBank: *HF969266*), from sequences and oligonucleotides communicated by Paula Irlles and Maria-Dolors Piulachs (unpublished results).

2.5. Windei depletion experiments

To knock-down BgWde, a dsRNA (dsBgWde) was prepared encompassing a 365 bp region starting at nucleotide 1919 of the BgWde sequence. The fragment was amplified by PCR and cloned into the pSTBlue-1 vector. As control dsRNA (dsMock), we used a 307 bp sequence from *Autographa californica* nucleopolyhedrovirus (GenBank: *K01149*, nucleotides 370–676) as in [18]. Preparation of the dsRNAs was performed as previously described [19]. Freshly emerged specimens from the last (6th) nymphal instar were treated with 1 µg of dsBgWde, injected into the abdomen in a volume of 1 µl of water-DEPC. Control specimens were treated similarly with 1 µg of

dsMock, or injected with 1µl of DEPC water to assess the absence of possible unspecific effects from dsMock injection.

2.6. Immunofluorescence and cell staining

Ovaries from 5-day-old adult females were dissected, fixed and processed as previously described [20]. Trimethylation of H3K9 was detected using a mouse monoclonal anti H3K9me3 antibody (Novus Biologicals 6F12-H4, Cambridge, UK) diluted 1:200. As secondary antibody an Alexa Fluor® 647-conjugated goat-anti-mouse IgG (Invitrogen™, Carlsbad CA, USA) diluted 1:400 was used. For F-actin visualization, ovaries were incubated with Phalloidin-TRITC (5µg/ml, Sigma) during 20 min. Ovarioles were mounted in UltraCruz™ Mounting Medium (Santa Cruz Biotechnology®, inc., Delaware CA, USA), which contains DAPI for DNA staining. Samples were observed by epifluorescence microscopy using a Zeiss AxioImager.Z1 microscope (Apo Tome) (Carl Zeiss MicroImaging).

2.7. Scanning electron microscopy (SEM)

Selected ovarioles from 7-day-old dsBgWde- and dsMock-treated females were processed to observe the chorion layers. Females were dissected late on day 7 of adult life in order to assess that chorion was completely formed in controls. Procedures were similar to those previously described [13], and after fixation with 2.5% glutaraldehyde in cacodylate buffer 0.2 M, oocytes were gently ripped with a microforceps in order to expose the layers. Samples were observed with a Hitachi S-3500N scanning electron microscope at 5 kV (Hitachi High-Technologies Corporation, Tokyo, Japan).

3. Results

3.1. The *Windei* ortholog of *Blattella germanica* (*BgWde*)

The cDNA of *B. germanica windei* was amplified, cloned and sequenced from ovarian tissues. The complete sequence is 4,675 bp long, with an ORF encoding for a

protein of 1,244 amino acids (nucleotide positions 13-3,678), with an estimated molecular mass of 135.8 kDa and an isoelectric point of 8.87. BLAST analysis of the protein sequence against databases revealed its homology with *D. melanogaster* Windei (Wde). Secondary structure prediction showed two coiled-coil regions and a C terminal fibronectin type III domain. Although the overall percentage of identity among the *D. melanogaster* Windei and the *B. germanica* sequence (BgWde) is only 17%, it reaches 47% within the fibronectin type III domain.

3.2. *BgWde* mRNA is highly expressed in the ovary

Using semi-quantitative PCR, we examined the expression of BgWde in the following adult female tissues: muscle, brain, digestive tract, colleterial glands, Malpighian tubules, fat body and ovary. BgWde is highly expressed in ovary (Fig. 1A) compared to expression in the digestive tract, colleterial glands or Malpighian tubules. BgWde expression was undetectable in the other tissues tested. Subsequently, the expression of BgWde mRNA in ovaries was measured by qRT-PCR during the gonadotrophic cycle. In the sixth (last) nymphal instar, BgWde mRNA levels are highest just after the molt (Fig. 1B), they decrease during the following days and then increase again just before the imaginal molt. In the adult stage, the highest expression is again observed during the first two days of adult life, but it then decreases steadily until oviposition.

3.3. *BgWde* depletion impairs ootheca formation and affects ovarian follicle growth

In order to unravel the BgWde function in oogenesis we followed an RNAi approach, treating freshly emerged sixth instar female nymphs with 1 µg of dsBgWde, 1 µg dsMock or 1 µl of DEPC water. Ovaries at different ages were dissected and the BgWde mRNA levels measured. BgWde transcript was depleted by a mean factor of 0.65 in 6-day-old sixth nymphal instar (N6D6) and by a mean factor of 0.42 in newly emerged adults (adult day 0, Add0), although differences were not statistically significant. In 5-day-old adult females (Add5) depletion was statistically significant

(0.555; $p < 0.008$), however, two days later, in 7-day-old females (AdD7), BgWde mRNA expression returned to normal levels (Fig. 1C).

To assess the role of BgWde in reproduction, 3-day-old adult specimens that had been treated either with dsBgWde or with dsMock were mixed with 7-day-old untreated adult males to facilitate mating. All dsMock-treated females ($n=23$) oviposited correctly and developed a well formed ootheca, while none of the dsBgWde-treated females ($n=34$) produced any ootheca. Indeed, 79.4% of the treated females did not oviposit at all, whereas the remaining 20.6% laid only 3-4 eggs that were dropped just thereafter, without forming the ootheca.

In order to study whether BgWde depletion affects ovarian follicle development, ovaries from females treated with dsBgWde or dsMock were examined at different ages. Ovaries from control and treated females were phenotypically indistinguishable at N6D6 and at AdD0. Ovarian follicles from AdD5 that had been treated with dsBgWde, had a slightly brown coloration, unlike the controls, which were completely white (supplementary Fig. 1A and B). Moreover, they were smaller than the controls: the average basal oocyte length in dsBgWde-treated ovaries was $955 \pm 215 \mu\text{m}$, which corresponds to oocytes from 3- to 4-day-old females, according to previous data [12], while dsMock oocytes presented a normal day 5 basal oocyte length (average length $1618 \pm 67 \mu\text{m}$) (Fig. 2A and B). Follicular cells were also smaller in dsBgWde-treated ovaries than in the controls and displayed signs of cytoskeleton disorganization, although they were binucleated, which is a characteristic feature of follicular cells from 5-day-old adult females (Fig. 2 C-E). Around 70% of AdD7 dsBgWde-treated ovaries were similar to the controls in size and shape, while 30% were smaller and browner. dsMock-treated females oviposited and formed the ootheca at the end of day 7 of the adult stage, as expected, while dsBgWde-treated females did not oviposit, as stated above. We dissected two of the dsBgWde-treated females at day 8 and found follicles with different lengths and shapes, but none appear to have chorion structures (Fig. 2 F and G). A 12-day-old dsBgWde-treated female showed the basal follicles fully vitellin mature, with a size and shape similar to the basal follicles of late day 7 control females, but again apparently without chorion and the colleterial glands perfectly formed (Supplementary Fig. 1C). Finally, we dissected two 20-day-old dsBgWde-treated

females and found that the basal follicles were round-shaped, white in color and a hole-type structure was observed in the middle (Fig. 2H).

3.4. BgWde depletion prevents chorion formation

According to the above observations and given that chorion is indispensable for ootheca formation [21], we suspected that the lack of oviposition (and ootheca formation) derived from anomalies in the chorion. Thus, we measured the mRNA levels of the following chorion genes by qRT-PCR: follicle cell protein 3C (Fcp3C) [14], yellow-g [14], citrus [13] and brownie [17]. Measurements were carried out in mid-chorion control follicles (dsMock treated) and in follicles from 7-day-old females that had been treated with dsBgWde. We also measured lipid storage droplet-2 (Lsd-2) mRNA levels as a positive control, because this gene is not related to choriogenesis and has a constant expression during the process (Paula Irlles and Maria-Dolors Piulachs, unpublished results). Results showed a complete depletion of mRNA levels in brownie, citrus and yellow-g ($p < 0.01$), and a down-regulation of Fcp3C by a mean factor of 0.009 ($p < 0.01$). As expected, mRNA levels in Lsd-2 were not significantly affected by the treatment with dsBgWde (Fig. 3A). To assess the absence of chorion structures in dsBgWde-treated females, we examined the basal ovarian follicle of treated and control, late day 7 females using SEM. Eggs from dsMock-treated females showed a properly formed chorion (Fig. 3B and C), with the different chorion layers easily distinguishable: inner endochorion, columnar layer and outer endochorion, as well as the exochorion. Conversely, none of the chorion layers were present in the basal oocyte of dsBgWde-treated females of the same age, at the end of the maturation cycle (Fig. 3D-F).

3.5. BgWde depletion reduces H3K9me3 in follicular cells

In *D. melanogaster*, the lack of Windei leads to reduced H3K9me3 in germ cells [8], which led us to question whether H3K9me3 was affected in the follicular cells of *B. germanica* that had been treated with dsBgWde. Therefore, we carried out an immunohistochemical study with an antibody against H3K9me3 in ovaries through the gonadotrophic cycle and, as in *D. melanogaster*, labeling was detected in the nuclei of

both oocyte and follicular cells. In relation of choriogenesis and focusing on the follicular cells, H3K9me3 labeling in 5-day-old dsBgWde-treated females was strongly reduced in comparison with dsMock-treated females. Indeed, only 21.7% of the treated ovarian follicles showed a labeling pattern similar to that of the controls, that is, with most of the cells labeled (ca. 90%), while the remaining 78.3% showed only 0-10 stained cells per ovarian follicle (Fig. 4A and B).

As H3K9me3 has been related to transcriptional repression [7], we analyzed the expression level of different mRNAs in ovaries from 5-day-old females. We selected genes involved in cell proliferation signaling pathways (hippo and yorkie from the Hippo pathway [22], notch, hindsight and cut from the Notch pathway [23]), genes controlling cell cycle (origin recognition complex (orc1), and cyclin E [24]), and Fcp3C, the only chorion gene expressed at day 5 in *B. germanica* [14]. Results indicated that all mRNAs studied were significantly overexpressed (Fig. 4C), with the exception of Fcp3C, which was significantly underexpressed.

4. Discussion

In the cockroach *B. germanica*, we have characterized a cDNA corresponding to an ortholog of *D. melanogaster* Windei (DmeWde) and mammalian mAM/MCAF1 (also known as ATF7IP) [25]. The corresponding proteins associate with histone lysine-methyl transferases (HKMTs), thus forming complexes that are involved in heterochromatin formation [7, 26]. Although proteins belonging to this group vary in their amino acidic sequence, they share a common domain structure, with at least one internal coiled-coil region and a C-terminal fibronectin type III repeat [8, 26]. We have named this new gene BgWde.

Depletion of BgWde mRNA by RNAi in *B. germanica* females prevents oviposition and ootheca formation, these effects being apparently derived from the absence of chorion layers provoked by the same treatment, as chorion formation is a pre-requisite for oviposition [21]; moreover, the colleterial glands, which are the main structure involved in the formation of the ootheca, were not affected by BgWde depletion. Chorion layers are produced by the follicular epithelium in the last stages of basal follicle maturation [27, 28] and genes encoding chorion proteins are highly

expressed during this period [14, 29]. Our SEM observations showed that BgWde knock down specimens do not form chorion layers, and qRT-PCR measurements indicated that typical chorion genes are not expressed when choriogenesis should take place, suggesting that chorion does not form because the genes involved in the process are not expressed.

In *D. melanogaster*, Wde has been described as a cofactor of Eggless, an HKMT that catalyzes H3K9me3 in ovarian somatic and germ cells [8, 9], this epigenetic mark being usually associated to transcriptional repression [30, 31]. We analyzed H3K9me3 in follicular epithelium of 5-days-old control and treated adult females and observed a significant reduction of H3K9me3 in the dsBgWde-treated group. This indicates that BgWde is needed for the trimethylation of H3K9 in the ovary of *B. germanica*, as occurs in *D. melanogaster*, which led us to propose that it acts as a cofactor of a putative *B. germanica* HKMT ortholog. We also analyzed the expression of several genes in ovarian follicles of adult day 5 females and we found a significant overexpression in almost all of them in the dsBgWde-treated group, which is coherent with the transcriptional repressor role of H3K9me3. The only transcript that was underexpressed in the dsBgWde-treated group was Fcp3C, which encodes a protein involved in the formation of the vitelline membrane, the first secreted chorion layer [14].

Taken together, our data reveal an essential role of BgWde in choriogenesis. As H3K9me3 generally acts as a transcriptional repression mark, we can speculate that there might be a repressor of chorion genes transcription that would become de-repressed upon BgWde depletion. Despite the fact that both Wnde1 and H3K9me3 have been detected in follicular cells in *D. melanogaster* [8, 9] this is the first time that a function for Wnde1 and H3K9me3 has been demonstrated in these cells. To our knowledge, this is also the first time that an epigenetic mark has been found to have a key role in choriogenesis, although further studies will be necessary to unravel the complete sequence of events that lead to the absence of chorion in BgWde expression depleted female cockroaches.

5. Conclusions

In the German cockroach, *B. germanica*, depletion of Winder by RNAi leads to a reduction of H3K9me3 in the epithelial follicular cells. This in turn triggers changes in transcriptional regulation that suppress the expression of chorion genes. This impairs oviposition (and, thus, ootheca formation) and prevents, therefore, reproduction.

Acknowledgements

Support for this research was provided by the Spanish Ministry of Science and Innovation (BFU2011-22404 to MDP and CGL2008-03517/BOS to XB), by the CSIC (grant 2010TW0019, Formosa program) and from FEDER funds to XB. Support from Generalitat de Catalunya (2005 SGR 00053) and LINC-Global is also gratefully acknowledged. AH received a pre-doctoral research grant (JAE-LINCG program) from the CSIC, and The European Social Fund (ESF). Thanks are also due to J. M. Fortuño (Centre Mediterrani d'Investigacions Marines i Ambientals, CSIC) for help with SEM studies, and to Dr. P. Irlles for her kindness in share the information of Hippo and Notch pathway.

References

- [1] E.L. Greer, Y. Shi, Histone methylation: a dynamic mark in health, disease and inheritance, *Nat Rev Genet* 13 (2012) 343-357.
- [2] S.L. Berger, The complex language of chromatin regulation during transcription, *Nature* 447 (2007) 407-412.
- [3] M. Lachner, R.J. O'Sullivan, T. Jenuwein, An epigenetic road map for histone lysine methylation, *J Cell Sci* 116 (2003) 2117-2124.
- [4] C. Martin, Y. Zhang, The diverse functions of histone lysine methylation, *Nat Rev Mol Cell Biol* 6 (2005) 838-849.
- [5] P. Cheung, P. Lau, Epigenetic regulation by histone methylation and histone variants, *Mol Endocrinol* 19 (2005) 563-573.
- [6] C. Seum, E. Reo, H. Peng, F.J. Rauscher, 3rd, P. Spierer, S. Bontron, *Drosophila* SETDB1 is required for chromosome 4 silencing, *PLoS Genet* 3 (2007) e76.
- [7] H. Wang, W. An, R. Cao, L. Xia, H. Erdjument-Bromage, B. Chatton, P. Tempst, R.G. Roeder, Y. Zhang, mAM facilitates conversion by ESET of dimethyl to trimethyl lysine 9 of histone H3 to cause transcriptional repression, *Mol Cell* 12 (2003) 475-487.
- [8] C.M. Koch, M. Honemann-Capito, D. Egger-Adam, A. Wodarz, Winder, the *Drosophila* homolog of mAM/MCAF1, is an essential cofactor of the H3K9

- methyl transferase dSETDB1/Eggless in germ line development, *PLoS Genet* 5 (2009) e1000644.
- [9] E. Clough, W. Moon, S. Wang, K. Smith, T. Hazelrigg, Histone methylation is required for oogenesis in *Drosophila*, *Development* 134 (2007) 157-165.
- [10] J. Yoon, K.S. Lee, J.S. Park, K. Yu, S.G. Paik, Y.K. Kang, dSETDB1 and SU(VAR)3-9 sequentially function during germline-stem cell differentiation in *Drosophila melanogaster*, *PLoS One* 3 (2008) e2234.
- [11] X. Wang, L. Pan, S. Wang, J. Zhou, W. McDowell, J. Park, J. Haug, K. Staehling, H. Tang, T. Xie, Histone H3K9 trimethylase Eggless controls germline stem cell maintenance and differentiation, *PLoS Genet* 7 (2011) e1002426.
- [12] X. Belles, J. Casas, A. Messegue, M.D. Piulachs, In vitro biosynthesis of JH III by the corpora allata of adult females of *Blattella germanica* (L), *Insect Biochemistry* 17 (1987) 1007-1010.
- [13] P. Irlles, M.D. Piulachs, Citrus, a key insect eggshell protein, *Insect Biochem Mol Biol* 41 (2011) 101-108.
- [14] P. Irlles, X. Belles, M.D. Piulachs, Identifying genes related to choriogenesis in insect panoistic ovaries by Suppression Subtractive Hybridization, *BMC Genomics* 10 (2009) 206.
- [15] A. Herraiz, F. Chauvigne, J. Cerda, X. Belles, M.D. Piulachs, Identification and functional characterization of an ovarian aquaporin from the cockroach *Blattella germanica* L. (Dictyoptera, Blattellidae), *J Exp Biol* 214 (2011) 3630-3638.
- [16] M.W. Pfaffl, G.W. Horgan, L. Dempfle, Relative expression software tool (REST) for group-wise comparison and statistical analysis of relative expression results in real-time PCR, *Nucleic Acids Res* 30 (2002) e36.
- [17] P. Irlles, X. Belles, M.D. Piulachs, Brownie, a gene involved in building complex respiratory devices in insect eggshells, *PLoS One* 4 (2009) e8353.
- [18] J. Lozano, X. Belles, Conserved repressive function of Kruppel homolog 1 on insect metamorphosis in hemimetabolous and holometabolous species, *Sci Rep* 1 (2011) 163.
- [19] L. Ciudad, M.D. Piulachs, X. Belles, Systemic RNAi of the cockroach vitellogenin receptor results in a phenotype similar to that of the *Drosophila* yolkless mutant, *FEBS J* 273 (2006) 325-335.
- [20] E.D. Tanaka, M.D. Piulachs, Dicer-1 is a key enzyme in the regulation of oogenesis in panoistic ovaries, *Biol Cell* 104 (2012) 452-461.
- [21] L.M. Roth, E.R. Willis, The Reproduction of the Cockroaches, *Smithsonian Miscellaneous Collections* 112, number 12 (1954).
- [22] G. Halder, R.L. Johnson, Hippo signaling: growth control and beyond, *Development* 138 (2011) 9-22.
- [23] J. Sun, W.M. Deng, Hindsight mediates the role of notch in suppressing hedgehog signaling and cell proliferation, *Dev Cell* 12 (2007) 431-442.
- [24] H.O. Lee, J.M. Davidson, R.J. Duronio, Endoreplication: polyploidy with purpose, *Genes Dev* 23 (2009) 2461-2477.
- [25] L. Liu, K. Ishihara, T. Ichimura, N. Fujita, S. Hino, S. Tomita, S. Watanabe, N. Saitoh, T. Ito, M. Nakao, MCAF1/AM is involved in Sp1-mediated maintenance of cancer-associated telomerase activity, *J Biol Chem* 284 (2009) 5165-5174.
- [26] T. Ichimura, S. Watanabe, Y. Sakamoto, T. Aoto, N. Fujita, M. Nakao, Transcriptional repression and heterochromatin formation by MBD1 and MCAF/AM family proteins, *J Biol Chem* 280 (2005) 13928-13935.
- [27] L.H. Margaritis, Structure and physiology of the eggshell, in: L.I. Gilbert, G.A. Kercut (Eds.), *Comprehensive Insect Physiology, Biochemistry and Pharmacology*, Pergamon Press, Oxford 1985, Vol. 1, pp. pp. 151-230.

- [28] X. Belles, P. Cassier, X. Cerda, N. Pascual, M. Andre, Y. Rosso, M.D. Piulachs, Induction of choriogenesis by 20-hydroxyecdysone in the German cockroach, *Tissue Cell* 25 (1993) 195-204.
- [29] A.C. Spradling, A.P. Mahowald, Amplification of genes for chorion proteins during oogenesis in *Drosophila melanogaster*, *Proc Natl Acad Sci U S A* 77 (1980) 1096-1100.
- [30] R.J. Klose, Y. Zhang, Regulation of histone methylation by demethylination and demethylation, *Nat Rev Mol Cell Biol* 8 (2007) 307-318.
- [31] R.J. Klose, K.E. Gardner, G. Liang, H. Erdjument-Bromage, P. Tempst, Y. Zhang, Demethylation of histone H3K36 and H3K9 by Rph1: a vestige of an H3K9 methylation system in *Saccharomyces cerevisiae*?, *Mol Cell Biol* 27 (2007) 3951-3961.

Figure Legends

Figure 1: Expression of BgWde mRNA in *Blattella germanica*. **A)** Expression in different tissues: muscle (Mu), brain (Br), digestive tract (DT) colleterial glands (CG), Malpighian tubules (MT), fat body (FB) and ovary (Ov); RT-PCR was performed with 3-day-old adult female tissues; expression of actin-5c was used as a reference. **B)** Expression pattern in the ovary during the last nymphal instar and the first reproductive cycle in the adult; qRT-PCR was performed using the expression of actin-5c as a reference; data represent copies of BgWde mRNA per 1000 copies of actin-5c mRNA, and are expressed as the mean \pm sem (n=3). **C)** Levels of BgWde mRNA in ovaries from dsBgWde-treated females; expression was measured in ovaries from 6-day-old sixth instar nymphs (N6D6) and in 0-, 5-, and 7-day-old adult females (Add0, Add5 and Add7, respectively); qRT-PCR data represent 3-4 biological replicates and are normalized against the control ovaries (water injected) (reference value=1); expression of actin-5c was used as a reference.

Figure 2: Effects of BgWde RNAi on ovarian follicle growth. **A)** Ovariole from 5-day-old dsMock-treated adult females. **B)** Ovariole from 5-day-old dsBgWde-treated adult females. **C)** Follicular epithelium of the basal follicle from 5-day-old dsMock-treated females. **D, E)** Follicular epithelium of the basal follicle from 5-day-old dsBgWde-treated females; actins (green) were stained with Phalloidin-TRITC, and DAPI was used to label the nuclei (blue). **F, G)** Ovarioles from 8-day-old dsBgWde-treated females. **H)** Ovary from a 20-day-old dsBgWde-treated female. Scale bar in A, B, F and G: 100 μ m; in C, D and E: 50 μ m; in H: 500 μ m.

Figure 3: Effects of BgWde RNAi on chorion formation. **A)** Expression of chorion genes: brownie, citrus, yellow-g and follicle cell protein 3C (Fcp3C) in ovaries of 7-day-old adult dsBgWde-treated females compared with dsMock-treated controls; lipid storage droplet-2 (Lsd-2) was used as a positive control; qRT-PCR data represent 4 biological replicates and are normalized against control ovaries (reference value=1); expression of actin-5c was used as a reference. **B, C)** Chorion layers in 7-day-old dsMock-treated females **D-F)** Absence of chorion in 7-day-old dsBgWde-treated

females; C: chorion, cl: columnar layer, ex: exochorion, FC: follicular cells, ie: inner endochorion, O: oocyte, oe: outer-endochorion, TP: tunica propria. Scale bar in B, D and E: 10 μm ; in C: 2 μm ; in F: 5 μm .

Figure 4: Effects of BgWde RNAi on H3K9me3 and gene expression. **A)** Follicular epithelium of the basal follicle from 5-day-old dsMock-treated females showing the H3K9me3 in the nuclei of follicular cells. **B)** Follicular epithelium of the basal follicle from 5-day-old dsBgWde-treated female showing the practical absence of H3K9me3 in the nuclei of follicular cells. H3K9me3 was revealed by immunofluorescence (magenta), actins (green) were stained with Phalloidin-TRITC, and DAPI was used to label the nuclei (blue). Scale bar: 20 μm . **C)** mRNA levels of hippo, yorkie, notch, hindsight, cut, orc1, cyclin E and follicular cell protein 3C (Fcp3C) in ovaries of 5-day-old adult dsMock and dsBgWde-treated females; qRT-PCR data represent 4 biological replicates and are normalized against control ovaries (reference value=1); expression of actin-5c was used as a reference; fold changes were statistically significant in all cases ($p < 0.05$).

Figure 1
[Click here to download high resolution image](#)

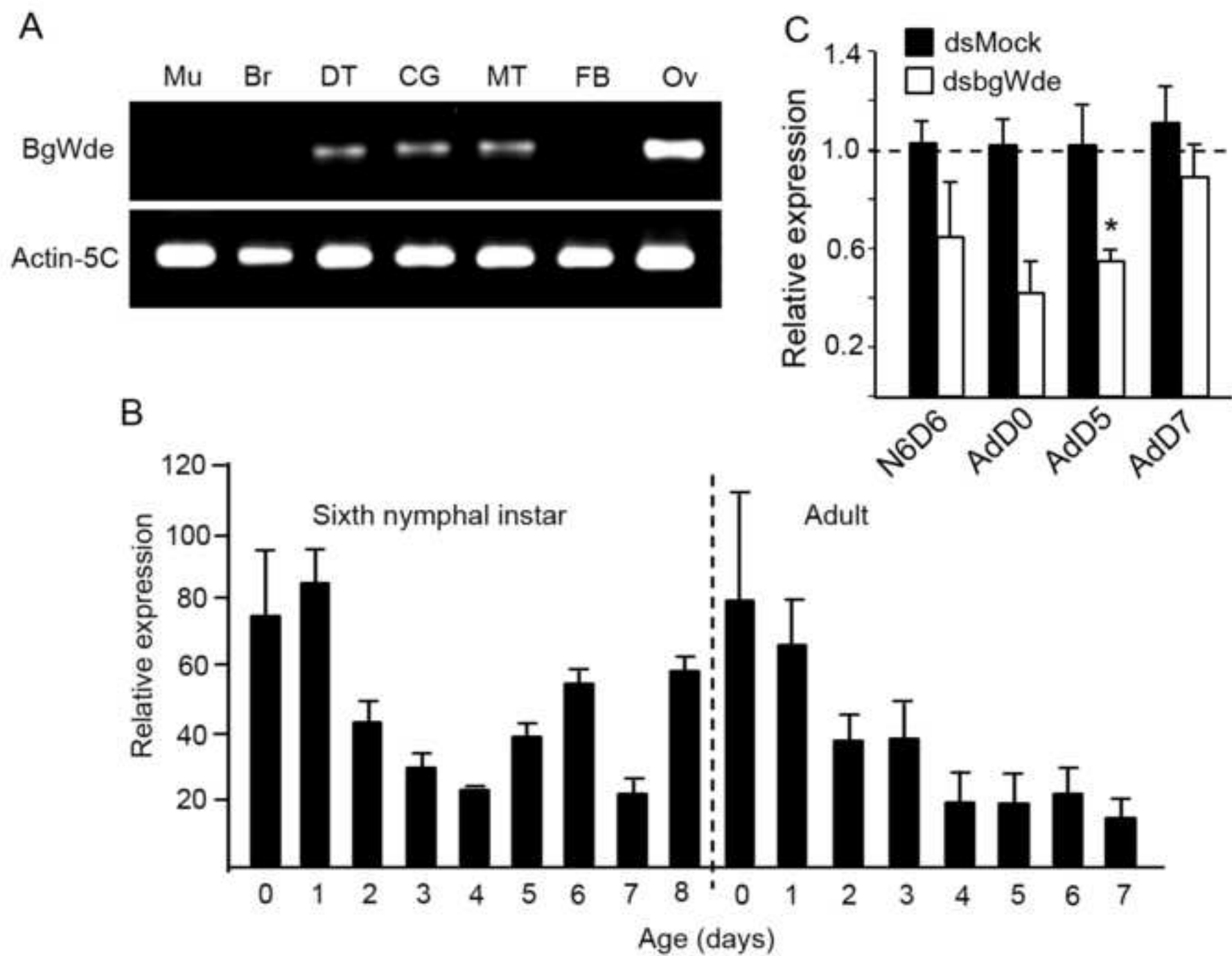


Figure 2
[Click here to download high resolution image](#)

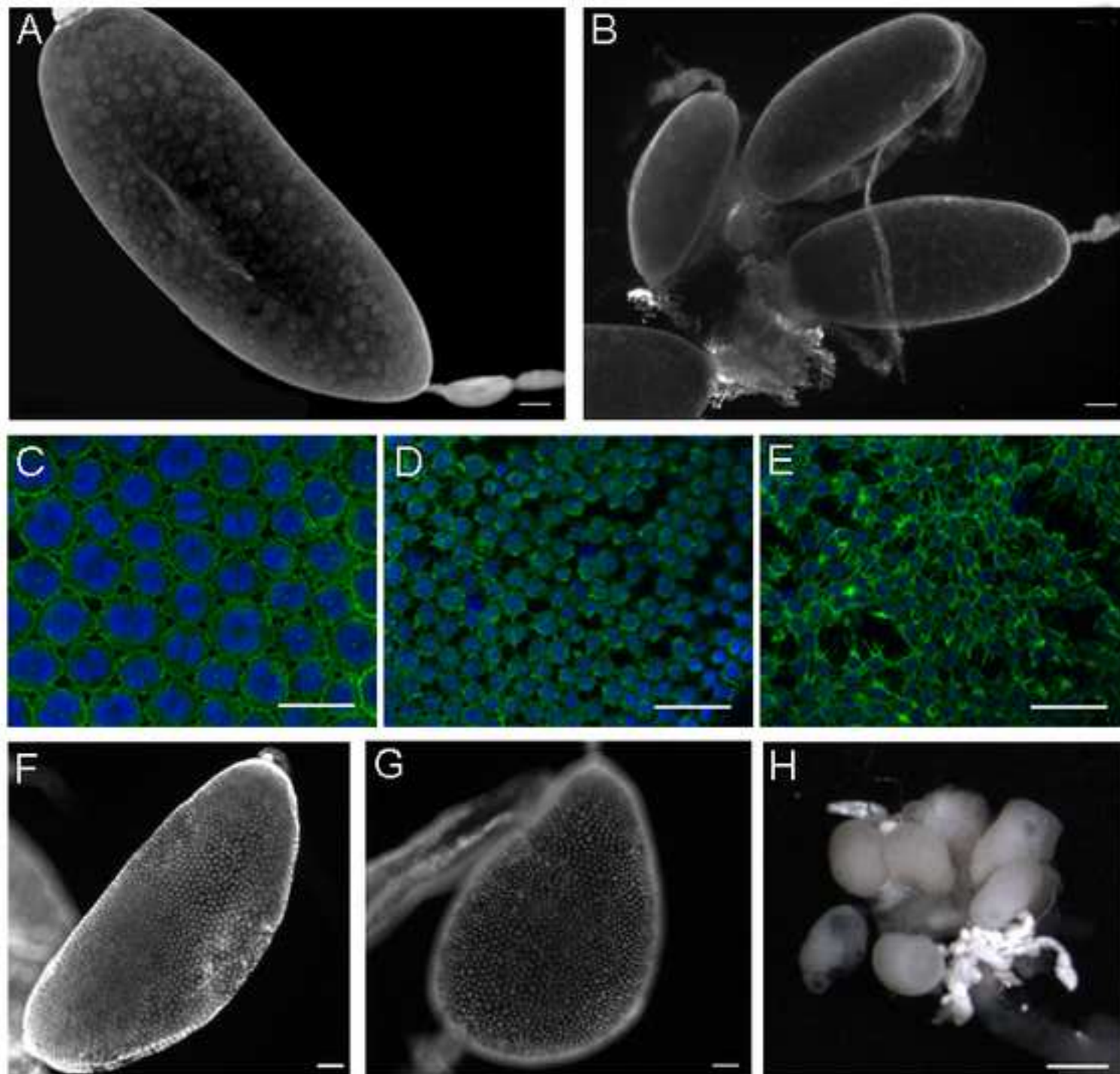


Figure 3
[Click here to download high resolution image](#)

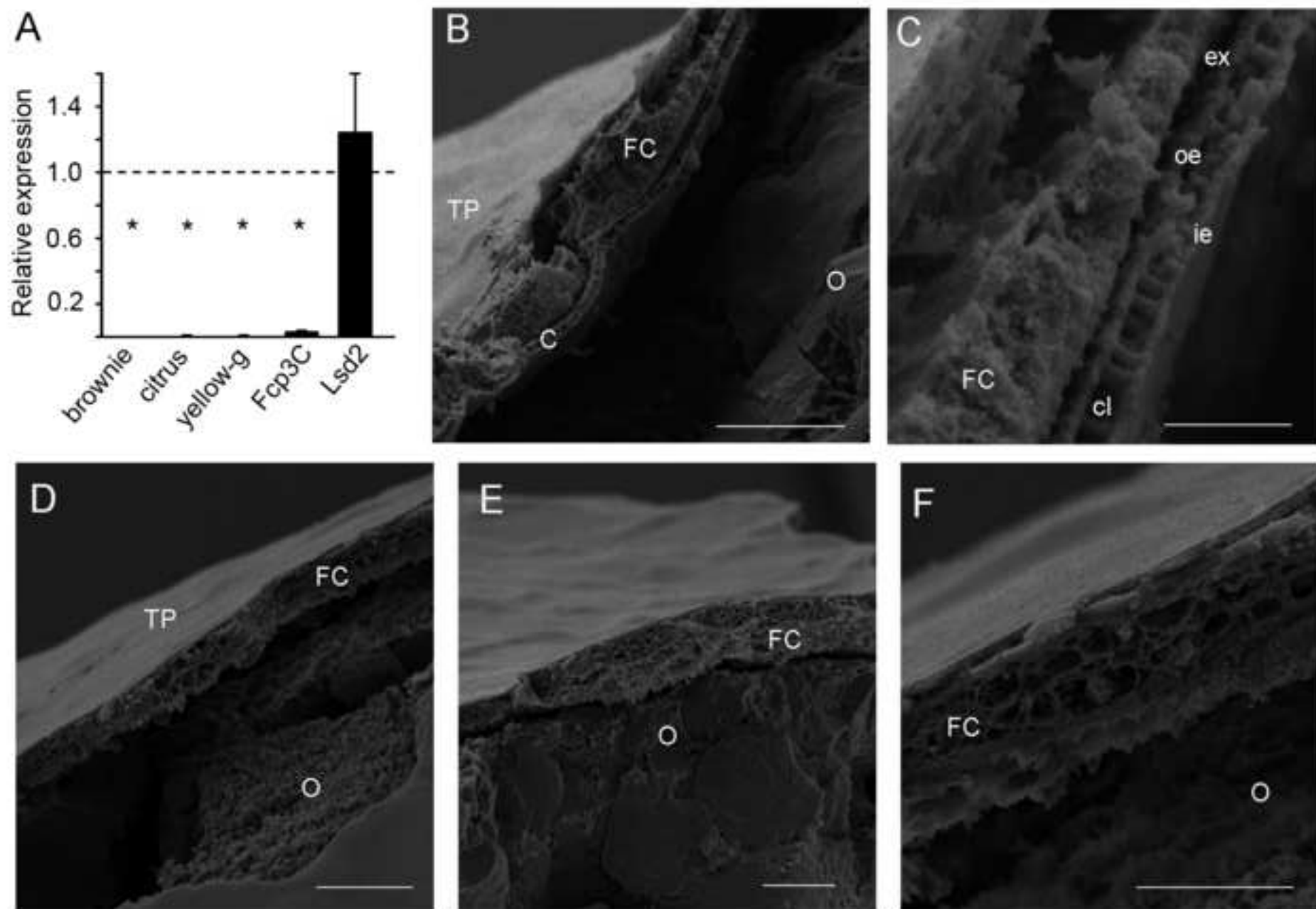
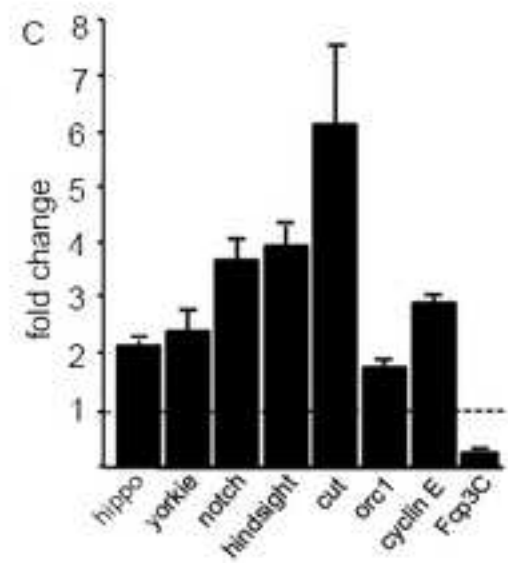
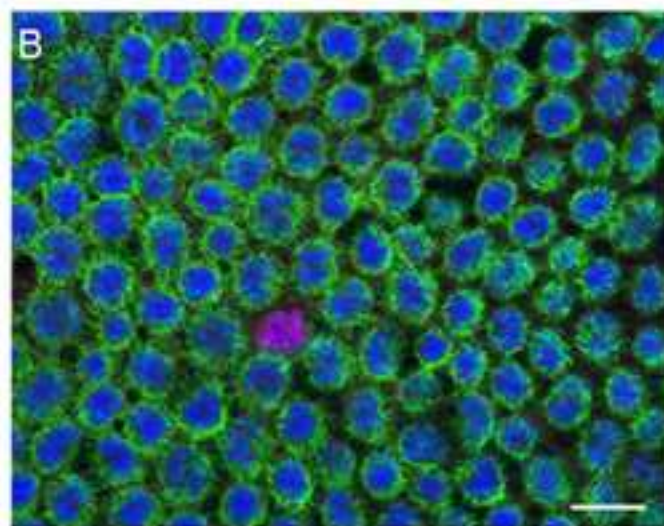
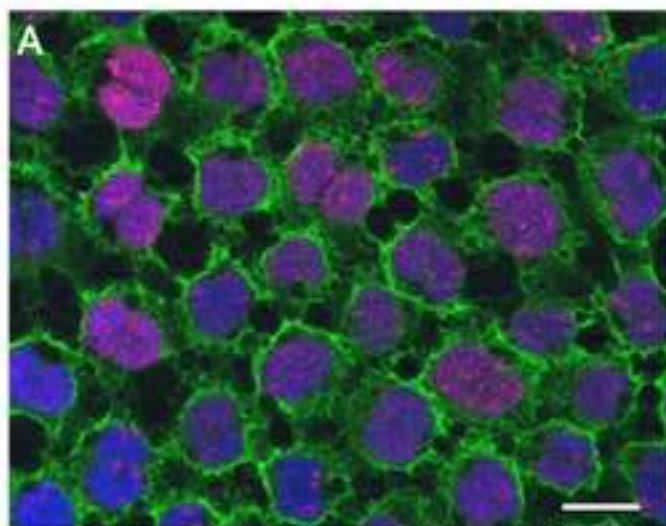


Figure 4
[Click here to download high resolution image](#)



Supplementary Table 1

[Click here to download Supplementary material for online publication only: Herraiz Supplementary Table 1.docx](#)

Supplementary Figure 1

[Click here to download Supplementary material for online publication only: Herraiz supplementaryFig1.tif](#)